Generation of Boundary Conforming Three-dimensional Anisotropic Meshes

Shayan Hoshyari

April 2016

Contents

1 Introduction

High-order accurate methods for simulation of fluid flow problems, are among the highly pursued research frameworks in Computational Fluid Dynamics, due to their potential to reduce the computational effort required for a given level of solution accuracy. My current thesis project is to generalize our in house high order turbulent viscous flow finite volume solver[4] to handle three dimensional geometries.

Conventional mesh generators create linear cells near the curved boundaries. However, high order numerical methods must account for the curved boundary in order to maintain their order of accuracy. For an isotropic mesh curving the faces on the boundary is sufficient. On the other hand, for anisotropic meshes, which are common in turbulent flow simulations, the mesh deformation should be propagated inside the domain to prevent unacceptable self intersecting elements.

To convert a three-dimensional anisotropic linear element mesh to a boundary conforming curved mesh, a solid mechanics analogy is used. The initial linear mesh is modeled as an elastic solid. When the boundary of the solid is deformed to match the curved boundary, the internal deformation of the solid will create the desired conforming curved mesh.

The equations modeling the elastic solid, i.e. Navier Equations, are written as[6]:

$$\nabla \cdot \sigma = 0 \tag{1}$$

Where σ is the symmetric three dimensional stress tensor and related to the displacement vector through the formulas :

$$
\begin{aligned}
\sigma_{11} &= (2\mu + \lambda)u_x + \lambda v_y + \lambda w_z \\
\sigma_{22} &= \lambda u_x + (2\mu + \lambda)v_y + \lambda w_z \\
\sigma_{33} &= \lambda u_x + \lambda v_y + (2\mu + \lambda)w_z \\
\sigma_{12} &= \mu u_y + \mu v_x \\
\sigma_{13} &= \mu u_z + \mu w_x \\
\sigma_{23} &= \mu v_z + \mu w_y
\end{aligned}
$$

Where u, v and w denote the components of the displacement vector, μ and λ are the Lame's coefficients, and the subscripts denote partial differentiation. The Lame's coefficients are among the properties of the solid, and will be considered constant throughout the domain.

This project deals with the solution of the system of equations (1) using the finite element method, as a starting step for a code that can convert linear mixed element three-dimensional meshes into curved boundary conforming ones. Based on our current two-dimensional mesh curving code we know that the Galerkin Method with C_0 cubic polynomial basis functions is a suitable approach to solve this system of equations, and that affine mappings will work for all the mesh elements, as the boundary of the initial domain is the actual linear mesh.

The libMesh[5] Library is used to implement the numerical method. libMesh is a C++ library that facilitates the implementation of many finite element methods in parallel. Internally, this library uses PETSc[1] to solve the large linear system of equations arising from discretizing the equations.

2 Numerical Method

The numerical method is constituted of two main parts, i.e., weak formulation of the problem, and the boundary conditions. Other parts, such as defining the basis functions, are automatically handled by the software library, and we only have to make the correct choice.

Discretized Weak Formulation

We are interested in the weak formulation of the system (1) with boundary conditions in the form:

$$\sigma\hat{n} + \mathbf{Q}(x)\mathbf{u} = \mathbf{t}(x) \tag{2}$$

Where $\hat{n}$ is the unit normal, the vector $\mathbf{t}$ and the matrix $\mathbf{Q}$ are only functions of spacial coordinates, and $\mathbf{u}$ is the displacement vector, i.e., $\mathbf{u} = (u, v, w)$. We will show that both the Dirichlet and Neumann boundary conditions can be implemented in this form.

The first step is to recast equation (1) into the following more convenient form:

$$
\begin{aligned}
-\nabla \cdot [\mathbf{K_{11}}\nabla u + \mathbf{K_{12}}\nabla v + \mathbf{K_{13}}\nabla w] &= f_1 \\
-\nabla \cdot [\mathbf{K_{21}}\nabla u + \mathbf{K_{22}}\nabla v + \mathbf{K_{23}}\nabla w] &= f_2 \\
-\nabla \cdot [\mathbf{K_{31}}\nabla u + \mathbf{K_{32}}\nabla v + \mathbf{K_{33}}\nabla w] &= f_3
\end{aligned} \tag{3}
$$

The functions f_i are identically zero except when a manufactured solution is used. The fourth order tensor $\mathbf{K}$ is defined as

$$K_{ijkl} = \lambda\delta_{ik}\delta_{jl} + \mu(\delta_{ij}\delta_{kl} + \delta_{il}\delta_{jk})$$

Where δ_{ij} is the Kronecker delta.

Now multiplying the first equation by a test function ϕ_i, integrating over the domain, and using the approximations $V = \sum_j U_j\phi_j$, $V = \sum_j V_j\phi_j$,and $W = \sum_j W_j\phi_j$ we will get the desired weak form.

$$\begin{aligned}
&\sum_j U_j \left(\int_\Omega \nabla\phi_i \cdot \mathbf{K}_{11}\nabla\phi_j + \int_{\partial\Omega} Q_{11}\phi_i\phi_j \right) + \\
&\sum_j V_j \left(\int_\Omega \nabla\phi_i \cdot \mathbf{K}_{12}\nabla\phi_j + \int_{\partial\Omega} Q_{12}\phi_i\phi_j \right) + \\
&\sum_j W_j \left(\int_\Omega \nabla\phi_i \cdot \mathbf{K}_{13}\nabla\phi_j + \int_{\partial\Omega} Q_{13}\phi_i\phi_j \right) \\
&= \int_\Omega f_1\phi_i + \int_{\partial\Omega} t_1\phi_i
\end{aligned} \tag{4}$$

The weak form of the second and third equations can also be found similarly, to form a linear system of equations $\mathbf{AU} = \mathbf{b}$.

Boundary Conditions

We are mostly interested in imposing the Dirichlet boundary condition on our boundaries to enforce the curved boundary conformity. We use the penalty method[2] for this job. In the penalty method the Dirichlet boundary condition is replaced by:

$$\sigma\hat{n} + \beta\mathbf{I}\mathbf{u} = \beta\mathbf{u}_D(x)$$

Which is equal to setting $\mathbf{Q} = \beta\mathbf{I}$ and $\mathbf{t} = \mathbf{u}_D(x)$. Where β is a huge number in the order of 10^{10}. Because of the machine rounding off errors, this condition will have the same result as directly enforcing $\mathbf{u} = \mathbf{u}_D(x)$. This method is especially convenient when basis functions other than Lagrange are used, where each degree of freedom will not necessarily correspond to the solution value at a certain point.

In other cases we might want to let the boundary move freely. This can be achieved by setting $\mathbf{Q}$ and $\mathbf{t}$ equal to zero.

Finishing Touches

After experimenting with the libraries' different options the following choices were made to be used in the solver code:

- The Lame' coefficients are found from the relations $\mu = E/(2(1+\nu))$ and $\lambda = (\nu E)/((1+\nu)(1-2\nu))$. ν is the Poisson's ratio, which is set to be 0.3. Due to our boundary conditions the Young's modulus, E cancels out of the equations (except for the manufactured solution case) so we simply choose the value of 1 for it.

- All the integrals are evaluated using the Gauss Quadrature formula of order $2p+1$ where p is the order of basis function polynomials.
- The linear system of equations is solved using the Conjugate Gradient method preconditioned with block ILU(2). It should be mentioned that PETSc's default matrix reordering method fails when cubic basis functions are used and a different method, e.g. the Reverse Cuthill-McKee (RCM), has to be used.
- libMesh supports three families of C_0 polynomials in three dimensions. Lagrange, Hierarchic[7] and Bernstein[3]. While all three expand the same function space, there are limitations in terms of library support. Also the stiffness of the linear system is different for each family. We will study this phenomenon in the results section.
- For simplicity all the problems will be solved using hexahedral meshes. When using quadratic basis functions the code can work with other element shapes as well. Cubic basis functions, on the other hand, are only supported for hexahedra in libMesh.

3 Results

The results are chosen slightly different from the project proposal. In the warm up stage the equations are solved in a simple box geometry and the accuracy is verified using a manufactured solution. In part A a real problem is solved and a linear mesh is actually curved. However, the geometry is simple which enables simple projection of points from the linear mesh boundary to the actual curved boundary. The geometry selected in Part B is chosen to mimic an actual three dimensional airfoil. Unlike the last part, projection of points onto the boundary is challenging and requires solving a nonlinear system of equations.

Manufactured solution in a box

A manufactured solution will be used to verify the accuracy of the implemented method. The geometry is a cube with unit sides while Dirichlet boundary conditions will be imposed on all the boundaries. The manufactured solution has the following form [1]:

$$\begin{aligned}
u &= \cos(\pi x)\cos(\pi y)\cosh(\pi z) \\
v &= \cos(\pi x)\cos(2\pi y)\cosh(\pi z) \\
w &= \cos(2\pi x)\cos(\pi y)\cosh(2\pi z)
\end{aligned}$$

The source terms f_i are subsequently calculated from equation (3) with the aid of maple.

The equations are solved on a series of refined meshes comprised of 5, 10 and 20 elements in each direction. Figure 1 shows the behavior of error norms with respect to mesh refinement. As expected the H^1 and L_2 norms are of order p and $p+1$ respectively. Where p is the order of basis function polynomials. This verifies the correct implementation of the numerical method and correct choice of quadrature accuracy. The results shown in Figure 1 are obtained using Hierarchical basis functions.

[1] I should confess that this is a poor choice for the manufactured solution especially due to the term $\sinh(2\pi z)$. This causes the solution to be too big at certain regions. $\cos(\sinh(z))$ would have been a better candidate.

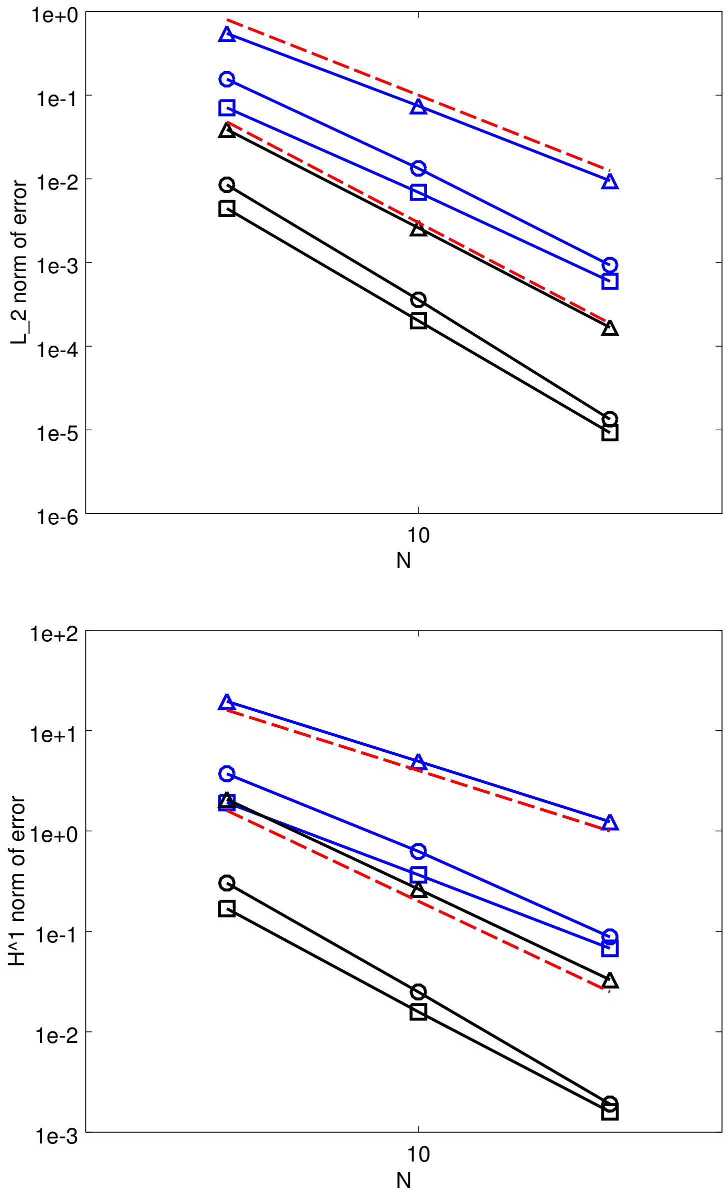

Figure 1: Norms of the error for the manufactured solution in a cubic domain. The blue lines are obtained by using quadratic basis functions while the black lines correspond to cubic basis functions. Triangles, Circles and Squares represent the error in u, v and w respectively. In the upper figure the red lines show third and fourth order reduction, whereas in the lower figure they represent second and third order reduction.

Curving an incomplete sphere mesh

The geometry of this problem is a wedge with inner and outer radii of 1 and 2 and arch length of $\pi/3$ revolved around the z axis which crosses the circle center and is perpendicular to one of the sides. The geometry and some parts of the initial linear mesh are shown in Figure 2.

In this problem we are only interested in conforming the inner surface of the incomplete sphere to the actual boundary. For any point on this surface we impose a Dirichlet boundary condition in the form of:

$$\mathbf{U}_D(x) = \frac{\mathbf{x}}{|\mathbf{x}|} - \mathbf{x}$$

Which will ensure that every point on the surface of the linear mesh will be moved to its projection on the original curved surface. The outer curved surface is held fix, i.e., $\mathbf{U}_D(x) = 0$. This is aimed to be an imitation of the far field boundary in an actual aerodynamic problem. Natural boundary conditions are imposed on the other boundaries (sides).

The displacement field obtained using quadratic Lagrange basis functions is shown in Figure 3. As expected the vertices of the original mesh are displaced only by a negligible amount (due to the penalty method for boundary conditions), while the midpoints of the elements are displaced the most. As we move in the radial direction towards the outer surface the displacement gets smaller and smaller as desired. Remember that we wanted the outer surface to stay intact.

We are also interested to study how the basis functions can affect the stiffness of the linear system and the convergence history. Figure 4 shows the convergence history for each case. It appears that the Bernstein polynomials create a much better conditioned system compared to the Hierarchic polynomials. Lagrange polynomials also perform well. However, their cubic version is not implemented in libMesh.

Curving a three-dimensional airfoil mesh

The geometry of this problem is shown in Figure 5. The bump in the middle, a poor man's version of an actual wing, is part of a circle which is extruded in the $4\hat{\jmath} + \hat{\imath}$ direction and resized simultaneously.

We are interested in making the mesh conforming to the surface of the airfoil. To do so we impose the following Dirichlet boundary condition on the airfoil surface.

$$\mathbf{U}_D(\mathbf{x}) = \text{Proj}(\mathbf{x}) - \mathbf{x}$$

Where $\text{Proj}(\mathbf{x})$ is the projection of the point $\mathbf{x}$ onto the airfoil surface, i.e., the line connecting $\mathbf{x}$ and $\text{Proj}(\mathbf{x})$ is perpendicular to the airfoil surface.

To find $\text{Proj}(\mathbf{x})$ we first parametrize the airfoil surface. Assuming $\mathbf{y}$ is a point on the surface we shall have

$$\mathbf{y} = \mathbf{y}(u, v)$$

Subsequently the normal at $\mathbf{y}$ is found to be

$$\hat{n}(u, v) = \frac{\mathbf{y}_u \times \mathbf{y}_v}{|\mathbf{y}_u \times \mathbf{y}_v|}$$

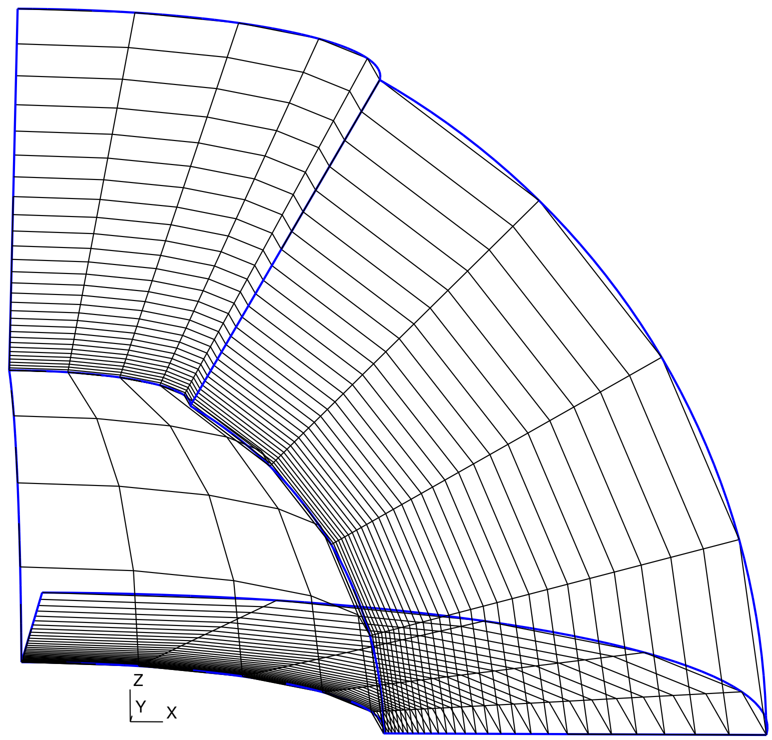

Figure 2: Geometry and the mesh for the incomplete sphere problem.

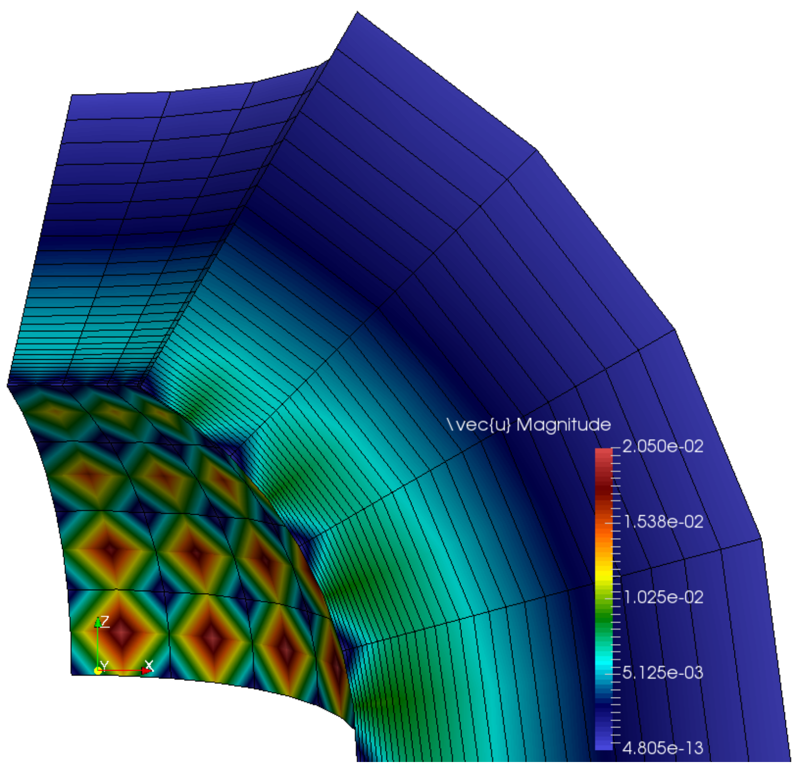

Figure 3: The displacement magnitude for the incomplete sphere case.

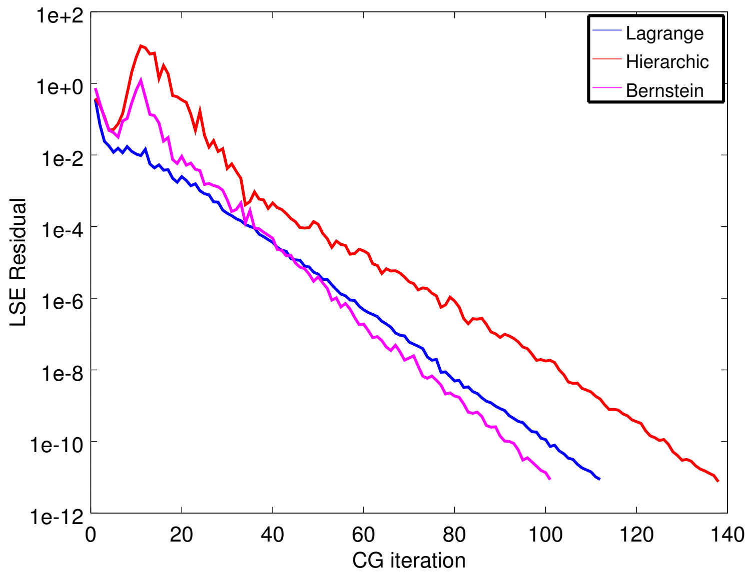

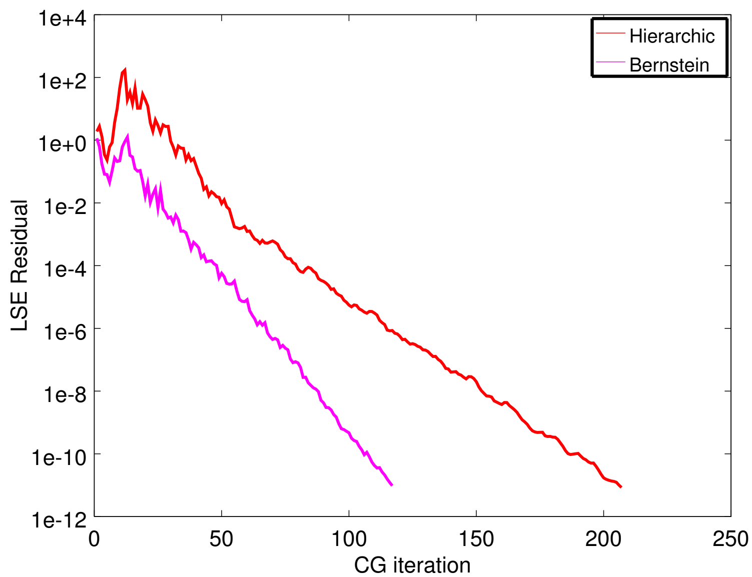

Figure 4: Convergence history for the incomplete sphere case. The upper and lower figures correspond to the quadratic and cubic basis functions respectively.

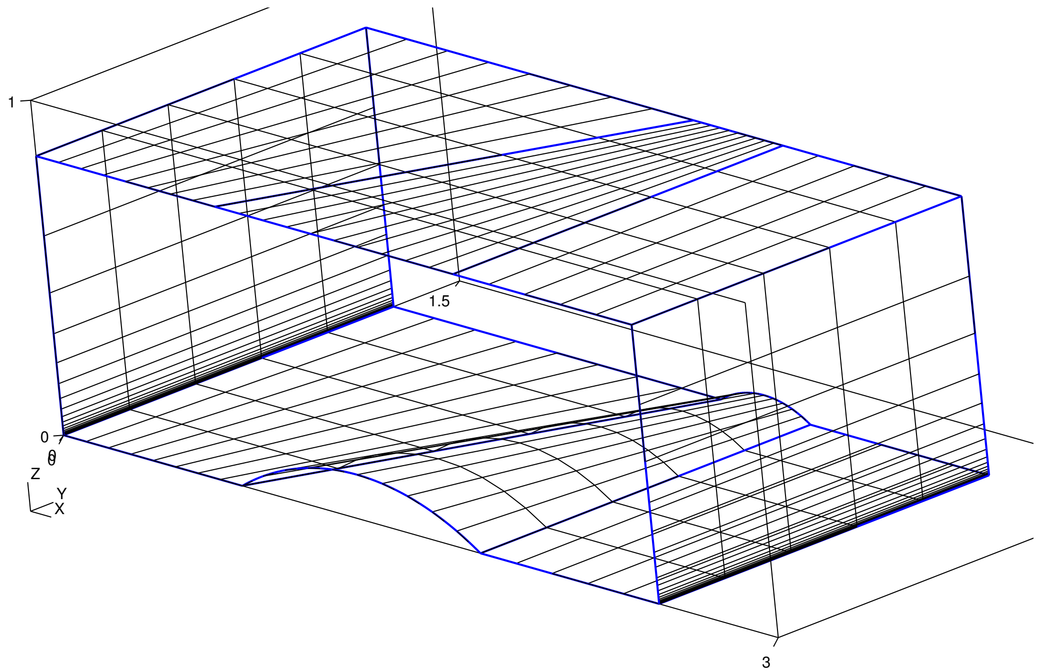

Figure 5: Geometry and the mesh for the airfoil problem.

Now to find $\mathrm{Proj}(\mathbf{x}) = \mathbf{y}$ we have to solve the following non-linear system of equations for u, v and d (the distance between x and y):

$$\mathbf{x} - \mathbf{y}(u, v) - d\hat{n}(u, v) = 0$$

This equation is solved using PETSc's non-linear solver, which is a combination of the Newton's method with finite difference Jacobian and the line search method, for every surface quadrature point.

For this particular case the surface parametrization reads as:

$$\mathbf{y}(u, v) = (u + (R_0 - bu)\sin(v), cu, (R_0 - bu)cos(v) - H_0(1 - \frac{bu}{R_0}))$$

$$0 < u < 1.25, \qquad -\frac{\pi}{6} < v < \frac{\pi}{6}$$

$$R_0 = 1, \qquad H_0 = \cos(\frac{\pi}{6}), \qquad b = 2, \qquad c = 4$$

For straight boundaries perpendicular to y and z axes the normal displacement is enforced to be zero while natural boundary condition is used for the tangent displacement. On the other hand, for the straight boundaries perpendicular to x axis free boundary condition is used for all displacement components. I am suspicious that if Dirichlet boundary conditions are used for all boundaries the system of equations maybe be ill-posed. Intuitively, this can be explained by the fact that the volume of the total solid cannot change arbitrarily.

Figure 7 shows the convergence history obtained by using different basis functions. Bernstein polynomials outperform their counterparts in this case as well. It is also noteworthy to mention that the residual tends to increase in the initial iterations except for Lagrange polynomials.

Figure 6 shows the displacement field obtained using quadratic Lagrange basis functions. Similar to the previous example problem the vertices of the original mesh are displaced negligibly, while the midpoints

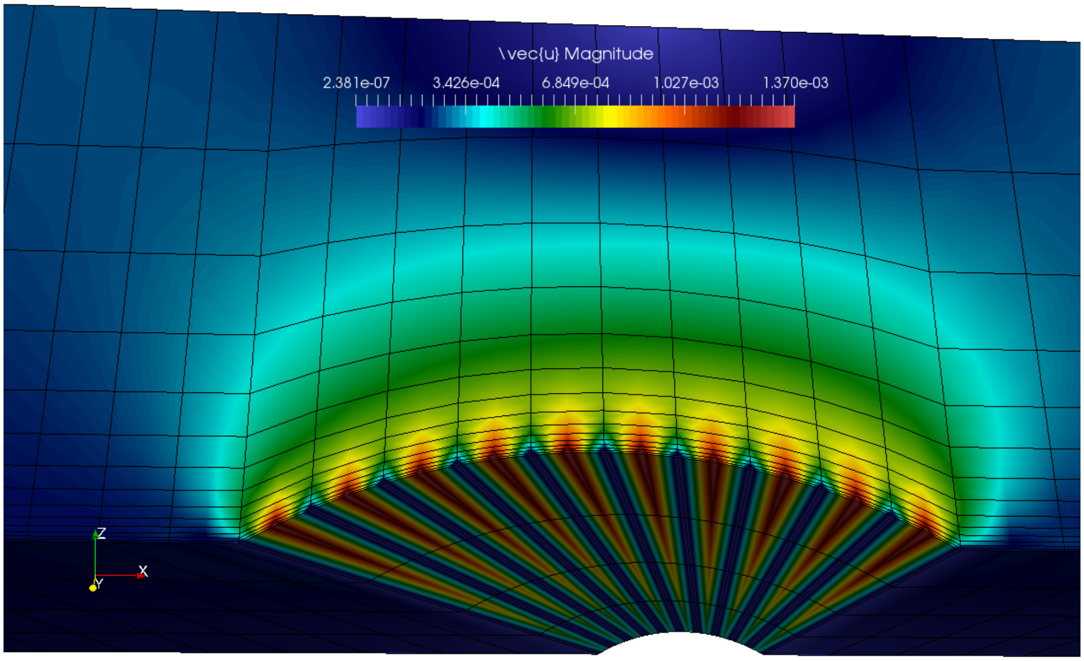

(a) Front view.

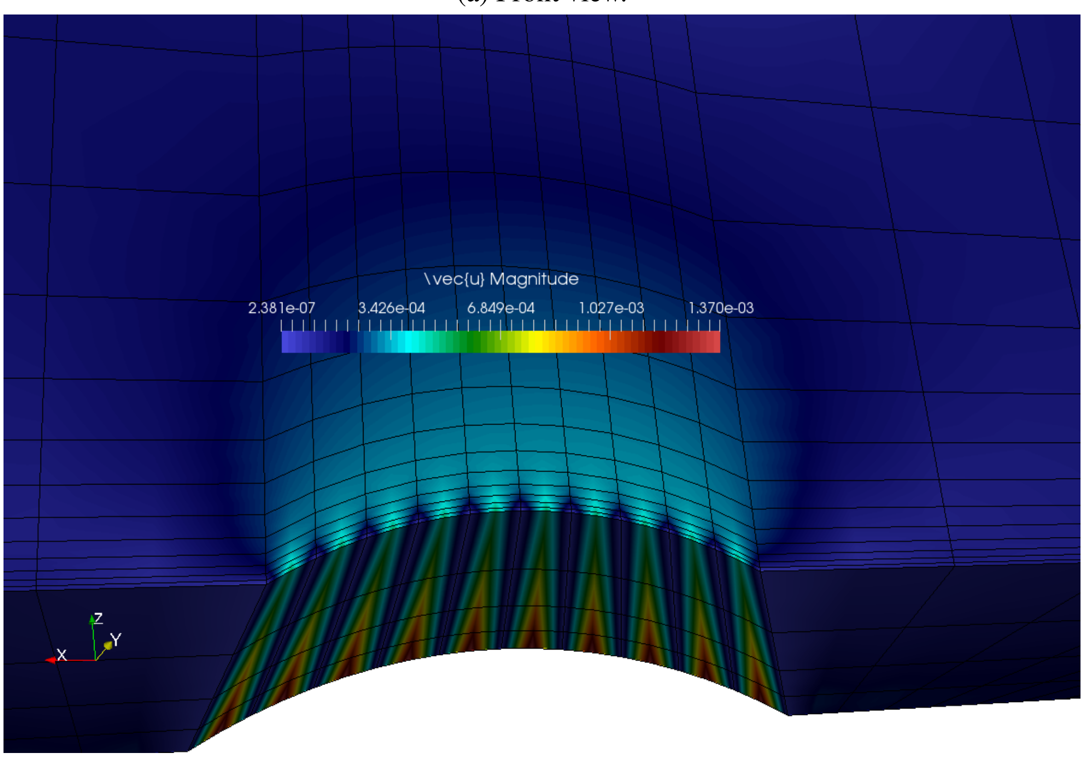

(b) Back view.

Figure 6: The displacement field for the airfoil case.

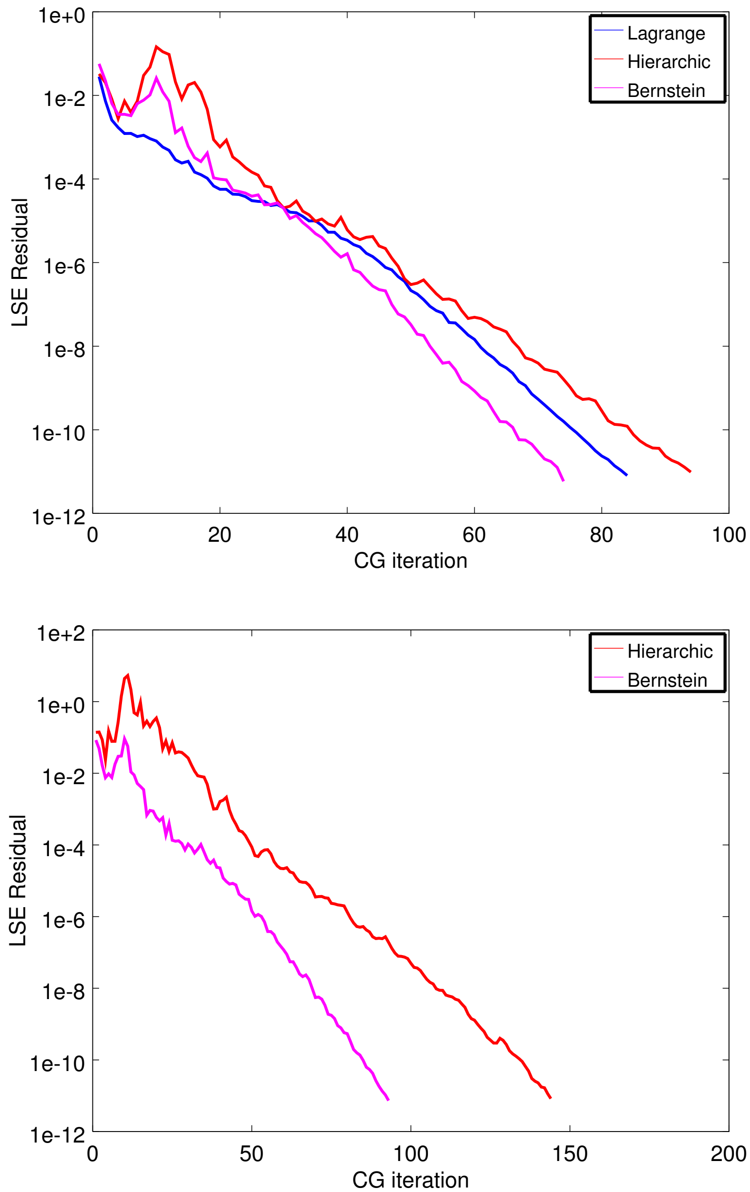

Figure 7: Convergence history for the airfoil case. The top and bottom figures correspond to the quadratic and cubic basis functions respectively.

of the elements are displaced the most. The displacement is propagated throughout the mesh, and tends to zero in the midway to the top and side surfaces.

References

[1] S Balay, S Abhyankar, M Adams, J Brown, P Brune, K Buschelman, V Eijkhout, W Gropp, D Kaushik, M Knepley, et al. Petsc users manual revision 3.5. Technical report, Technical report, Argonne National Laboratory (ANL), 2014.

[2] Eric Becker, Graham Carey, and J Oden. Finite elements. an introduction. 1981.

[3] Rida T Farouki and VT Rajan. On the numerical condition of polynomials in bernstein form. *Computer Aided Geometric Design*, 4(3):191–216, 1987.

[4] Alireza Jalali and Carl Ollivier Gooch. Higher-order unstructured finite volume methods for turbulent aerodynamic flows. In *22nd AIAA Computational Fluid Dynamics Conference*, page 2284. 2015.

[5] Benjamin S Kirk, John W Peterson, Roy H Stogner, and Graham F Carey. libmesh: a c++ library for parallel adaptive mesh refinement/coarsening simulations. *Engineering with Computers*, 22(3-4):237–254, 2006.

[6] W Michael Lai, David H Rubin, David Rubin, and Erhard Krempl. *Introduction to continuum mechanics*. Butterworth-Heinemann, 2009.

[7] Olgierd Cecil Zienkiewicz, Robert Leroy Taylor, Olgierd Cecil Zienkiewicz, and Robert Lee Taylor. *The finite element method*, volume 3. McGraw-hill London, 1977.